

Coherence creation in an optically thick medium by matched propagation of a chirped-laser-pulse pair

N. Sandor, G. Demeter, D. Dzsotjan, and G. P. Djotyan

Wigner Research Center for Physics, Hungarian Academy of Sciences, Konkoly-Thege Miklós út 29-33, H-1121 Budapest, Hungary

(Received 1 March 2013; published 12 March 2014)

We consider the simultaneous propagation of a pair of Raman-resonant, frequency-modulated (chirped) laser pulses in an optically thick medium, modeled by an ensemble of Λ atoms. A self-organization (“matching”) effect is shown for the chirped-pulse pair, which leads to a quasilossless propagation. Furthermore, we demonstrate that a well-defined coherent superposition of the atomic ground states and, correspondingly, a coherence are robustly created in the medium that can be controlled by amplitudes of the laser pulses. The proposed scheme can be applied to substantially increase the efficiency of the optical wave mixing processes, as well as in other nonlinear processes where the initial preparation of a spatially extended medium in a coherent superposition state is required.

DOI: [10.1103/PhysRevA.89.033823](https://doi.org/10.1103/PhysRevA.89.033823)

PACS number(s): 42.50.Gy, 42.25.Bs

I. INTRODUCTION

Adiabatic control (AC) of atomic quantum states (see [1–3] and references therein) is a powerful technique in quantum optics that allows various applications in nonlinear optics, such as high harmonic generation [4], multiphoton ionization [5], nonlinear frequency conversion [6,7], and several transparency effects [8]. The general aim of AC is to create a given population distribution among the working levels of atomic systems in a robust way using a limited number of laser pulses.

One important control problem is the creation of coherence between specific states of single atoms or—allowing more exciting applications—ensembles of atoms. It has been shown [9] that preparing an optically thick medium of Λ atoms (see Fig. 1) in the coherent superposition of their ground states leads to numerous interesting phenomena. These include lasing without inversion [10,11], enhanced index of refraction of the medium [12,13], Ramsey interference [14], or enhancement of magneto-optical effects [15,16].

In our present paper, we propose a method for achieving this task by using a pair of frequency chirped (FC) laser pulses. We anticipate that the presented method allows a relatively precise control of the final state of the medium and is easier to apply in certain experimental situations than other methods known in the literature [17]. The problem of the preparation of an extended medium naturally raises the question of whether a lossless propagation of a pair of FC pulses is possible in the medium and, if so, by what mechanism? In this paper, we wish to give a detailed response to these questions.

The essence of AC is adiabatically tuning one of the parameters of the atom-laser interaction in time, which drives the atomic populations along the adiabatic states of the system [18,19]. If the evolution takes place along the dark state (population trapping), complete population control can be achieved without excitation of the atom. This mechanism is the basis of the stimulated Raman adiabatic passage (STIRAP) [20–23]. In the AC schemes based on STIRAP, two (or more) time-shifted laser pulses with constant carrier frequencies are applied to a quantum system, resulting in adiabatic altering of couplings between the laser fields and the atomic transitions.

FC laser pulses applied in the atom-laser interaction represent another possibility for performing AC. In this

case, the frequency of the driving electromagnetic field(s) is the key parameter governing the rearrangement of the atomic population among its quantum states. Although perfect population trapping in ground states cannot be realized when AC is performed by FC pulses (such as in the STIRAP-based schemes), numerous AC schemes were proposed with negligible atomic excitation [24–27].

The above-mentioned works generally concentrate on AC in single atoms and neglect the backaction of the atoms on the laser fields along with other propagation effects, such as the interaction of the laser pulses with each other. The latter effects, however, have to be taken into account when AC is performed in an optically thick medium [17,28–30]. In this case, preparation of the atoms of a medium in coherent superposition of the quantum states may significantly modify its optical properties, leading to very interesting and important propagation effects.

Most works in the literature deal with the propagation of transform-limited laser pulse(s) (without modulation of their frequency over time). In the (most known) case of electromagnetically induced transparency (EIT) (see [31–33] and references therein), an intense laser pulse (of constant carrier frequency) renders the whole medium transparent for a weak probe pulse in Raman resonance with the intense one. In these schemes, no population redistribution occurs in the first order.

Nearly lossless propagation was demonstrated in the case of constant-frequency pulses having identical [34] and complementary pulse envelopes [35] in optically thick media consisting of Λ atoms. In the above-mentioned schemes, the lossless propagation of the electromagnetic field(s) was ensured by initially preparing the medium in a dark superposition of the ground states. This means that no excitation occurs in the atoms during the interaction, which significantly reduces the backaction of the atoms on the laser field. As a result, basically the same population-control mechanism was established in the atoms of the extended medium as in a single atom, even for significant propagation distances.

On the other hand, it has been shown in [36] that for a sufficiently intense laser-pulse pair having constant frequencies in Raman resonance, lossless propagation is possible in

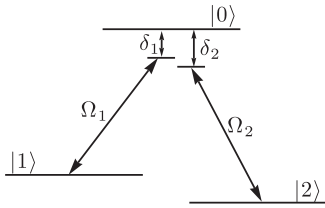


FIG. 1. Level scheme of the Λ atom. The dipole-allowed transitions (between the excited state $|0\rangle$ and the lower metastable states $|1\rangle$ and $|2\rangle$, respectively) are each coupled by a frequency-modulated (i.e., FC) laser pulse. In this paper, we consider Raman-resonant coupling, i.e., $\delta_1 = \delta_2 = 0$.

a medium of Λ atoms even if the initial preparation of the atoms does not coincide with the dark state. The explanation is that the laser pulses become distorted by the interaction with the medium in such a way that the initial preparation of the atoms corresponds to a dark state for the pulse pair after propagating some distance. In this sense, the interacting laser pulses become *matched* to each other through the interaction with the atoms of the medium.

The propagation of FC pulses in an extended medium, however, is less studied. In our earlier works ([37] and [25]), we considered several interaction schemes including Λ atoms and FC pulses. Comparing the schemes presented there, one may conclude that the population transition process induced among the states of the Λ atom depends on whether the coupling of the two ground states are in Raman resonance. That is, it was shown in [25] that a nearly excitation-free population transfer may be established among the ground states with a single FC pulse which can couple both of the transitions, provided that there is an energy difference between them (i.e., there is a Raman detuning between the couplings). Based on this scheme, the possibility of the quasilossless propagation of a single FC was shown [29].

The action of a pair of strong Raman-resonant FC pulses on a single atom results in adiabatic excitation of the bright component of the superposition of the ground states, leaving intact the dark component of this superposition [37]. As a result, a coherent superposition of the ground states is robustly created along with excitation of the atom. This excitation, however, is detrimental for the created coherence: One has to transfer the population of the excited state to another ground state to preserve the created coherence from the destructive effect of the spontaneous decay.

In the present investigation, we show that the Raman-resonant FC pulse pair, which would cause large excitation in a single atom, is modified by the medium in such a way that it no longer causes any significant excitation, and induces a coherent redistribution of the populations among the ground states of the atoms of the medium. It turns out that the matched propagation of the FC pulse pair possesses an important feature which is not typical for the matched propagation of pulses with constant carrier frequencies. Namely, the FC pulse pair, while propagating in a quasilossless way in the medium, prepares its atoms in a well-defined superposition of the metastable ground states. The created coherent superposition can be controlled by the peak amplitudes of the interacting laser pulses. The robust creation of (maximum) coherence between the ground

states of the atoms in an extended optically thick medium for applications in nonlinear frequency conversion processes is an important motivation of this investigation.

The paper is organized as follows. In Sec. II, a semiclassical model is presented for describing the interaction of the classical FC pulse pair with the optically thick medium composed of Λ atoms. We present our results in Sec. III. We analyze the behavior of the atomic states and the interacting laser-pulse pair in a transformed (symmetric-antisymmetric) basis at the boundary and inside the medium in Secs. III A and III B, respectively, based on numerical calculations and also by using the adiabatic approximation. We discuss our results in the original basis in Sec. III C, comparing them with the case of the propagation of a constant-frequency pulse pair. Our findings are summarized in Sec. IV.

II. MATHEMATICAL MODEL

We use a semiclassical approach for studying the propagation of the FC pulses in a medium of Λ atoms: the internal electronic state of the atoms is treated in the frame of quantum mechanics, while the laser pulses are described by the classical electric field,

$$\vec{E}(x,t) = \sum_{i=1}^2 \vec{\varepsilon}_i [\mathcal{E}_i(x,t) e^{-i(\omega_i t - k_i x)} + \text{c.c.}]. \quad (1)$$

The propagation of this field is given by the classical Maxwell equations. In Eq. (1), \mathcal{E}_i is the complex field amplitude of the i th laser pulse, which changes slowly in time and space compared to the frequency ω_i and wave number k_i ($i \in \{1,2\}$). The propagation of the pulses is considered in one direction. The central frequencies of the laser pulses are given by ω_i . In what follows, we assume that the pulses on the input boundary of the medium have the same linear frequency modulation (chirp), the range of which is much smaller than the transition frequencies. This allows us to incorporate the chirp into the slowly varying complex field amplitude \mathcal{E}_i as a time-dependent phase: $\mathcal{E}_i \sim \exp(i\beta t^2)$, with β being referred to as the “speed of the chirp.”

The medium in which this pair of classical FC pulses propagates is modeled by identical, noninteracting, and motionless atoms, which are all initially prepared in one of their internal ground states (for example, in state $|2\rangle$). We divide the medium into small segments, inside which we can neglect the backaction of the atoms on the electric field. Since the dipole-allowed transitions between two metastable states and a common excited state are quasilosslessly driven, the atom can be described on the Hilbert space spanned by the energy eigenstates (bare states) $\{|0\rangle, |1\rangle, |2\rangle\}$ with λ -type linkages (Fig. 1), where each pulse couples one transition. In our model, the difference of the transition frequencies is small, thus $\omega_1 \approx \omega_2$ and $k_1 = k_2 = k_x$ hold for the central frequencies and wave numbers of the coupling laser pulses. This coupling scheme may be realized by an $F = 1 \rightarrow F' = 0$ transition in an atom interacting with two laser pulses having σ^+ and σ^- polarizations.

The interaction of an arbitrary atom localized in the region $[x, x + \delta x]$ with the laser pulses is described in the rotating

wave approximation (RWA) [38] by the Hamiltonian

$$\hat{H}(x,t) = -\hbar \sum_{k=1}^2 [-\delta_k |k\rangle\langle k| + (\Omega_k(x,t)|0\rangle\langle k| + \text{H.c.})], \quad (2)$$

where

$$\Omega_k(x,t) = \frac{\mathcal{E}(x,t)d_{0k}}{\hbar} \equiv |\Omega_k| e^{i\phi_k(x,t)}, \quad k \in \{1,2\}, \quad (3)$$

is the Rabi frequency of the k th laser pulse, with the change of the frequency caused by the chirp included in the phase $\phi_k(x,t)$. $d_{0k} = \langle 0|\hat{d}|k\rangle$ is the matrix element $(0,k)$ of the dipole operator \hat{d} , whereas δ_k is the detuning of the central frequency (ω_k) of the k th pulse from the transition frequency between states $|0\rangle \leftrightarrow |k\rangle$. Here we consider a case where these ‘‘central detunings’’ are equal ($\delta_1 = \delta_2$), which we now set to be zero for the sake of simplicity. Note that the frequency modulation of both pulses entering the medium follows the same time dependence at the boundary of the medium. Therefore, at the boundary of the medium, the differences between the pulses’ instantaneous frequencies and the corresponding atomic transition frequencies are equal in every time point, i.e., the pulses which enter the medium are in ‘‘Raman resonance’’ with the atoms.

For later convenience, it is worth introducing $\xi = x/\xi_0$ and $\tau = (t - x/c)/\tau_\sigma$ dimensionless, space- and retarded-time coordinates. The time is measured in the unit of τ_σ , which characterizes the duration of the pulses. For the normalization of the space coordinates, we introduce the absorption length of a laser pulse of constant frequency ω_L in a medium consisting of resonant two-level atoms with a density of \mathcal{N} , which is given by [38]

$$\xi_0 = \frac{\epsilon_0 \hbar c}{\mathcal{N} \omega_L |d_A|^2 T}, \quad (4)$$

where T is the natural lifetime of the excited state and d_A is the dipole momentum of the coupled atomic transition. Although there are two atomic transitions in the present case, it is consistent with our previous approximations to regard a common absorption length for both coupling pulses by setting $|d_{01}| = |d_{02}| = d_A$, $\omega_L = (\omega_1 + \omega_2)/2$, and $T = 2/\Gamma_1 = 2/\Gamma_2 = 2/\Gamma$, where Γ_i is the longitudinal relaxation rate from the excited state $|0\rangle$ to the metastable state $|i\rangle$, $i \in \{1,2\}$.

We describe the response of the atoms for the ingoing laser radiation inside a certain space interval by the master equation

$$\begin{aligned} \partial_\tau \hat{\rho}(\xi, \tau) = & \frac{1}{i\hbar} [\hat{H}(\xi, \tau), \hat{\rho}(\xi, \tau)] - 2\Gamma |0\rangle\langle 0| \rho_{00}(\xi, \tau) \\ & + \sum_{k=1}^2 \{ \Gamma \rho_{00}(\xi, \tau) |k\rangle\langle k| - [\Gamma \rho_{0k}(\xi, \tau) |0\rangle \\ & \times \langle k| + \text{H.c.}] \} (\rho_{kl} = \langle k|\hat{\rho}|l\rangle), \end{aligned} \quad (5)$$

where the density matrix as a function of the space coordinate ξ is defined by the average

$$\hat{\rho}(\xi, \tau) = \frac{1}{N} \sum_{i=1}^N \hat{\rho}^{(i)}(\tau). \quad (6)$$

Here, N is the number of the atoms inside the space interval $[\xi, \xi + \delta\xi]$ and $\rho^{(i)}$ denotes the density matrix of the i th atom.

Since the change in the electromagnetic field is neglected inside a small segment, the Hamiltonian $\hat{H}(\xi, \tau)$ which drives the evolution of the average density operator is formally the same as in Eq. (2).

The atoms of the medium may affect the propagating laser pulses by means of basically two mechanisms: by spontaneous emission from the excited state and by dipole radiation [36]. Here we put emphasis on the latter by regarding a weakly decaying limit, where the lifetime of the excited state is assumed to be about an order of magnitude longer than the interaction time. The macroscopic polarization induced in the medium by the laser fields may be written as

$$\vec{P}(\xi, \tau) = N \text{Tr} \hat{\rho}(\xi, \tau) \hat{d} = N \sum_{k=1}^2 [\rho_{0k}(\xi, \tau) d_{0k} + \text{H.c.}]. \quad (7)$$

This quantity serves as a source in the Maxwell equation which is used to describe the dynamics of the electric field. Consistent with the RWA, one can apply the slowly varying envelope approximation [39] in order to get a first-order differential equation for the propagation from the second-order wave equation. Using these approximations, one gets the following differential equations for the Rabi frequencies of the laser pulses [see Eq. (3)]:

$$\frac{\partial}{\partial \xi} \Omega_k(\xi, \tau) = -i\alpha \rho_{k0}(\xi, \tau), \quad k \in \{1,2\}, \quad (8)$$

where $\alpha = \tau_\sigma/(2T)$ describes the strength of the coupling between the medium and the lasers.

Equations (5) and (8) together form a system of partial differential equations, which describes the coupled laser-atom system in the extended medium. In order to study the behavior of the propagating FC pulses and the atomic transitions induced by the laser field, we solve this system numerically. We use the following boundary conditions of two Gaussian, linearly chirped pulses entering the medium at $\xi = 0$ [see Fig. 2(a)]:

$$\begin{bmatrix} \Omega_1(\xi = 0, \tau) \\ \Omega_2(\xi = 0, \tau) \end{bmatrix} = \begin{bmatrix} \vartheta_1 \\ \vartheta_2 \end{bmatrix} e^{-\tau^2(\frac{1}{2} + i\beta)}, \quad \vartheta_k \in \mathbb{R} \quad \forall k \in \{1,2\}, \quad (9a)$$

$$\hat{\rho}(\xi, \tau \rightarrow -\infty) = |2\rangle\langle 2|, \quad (9b)$$

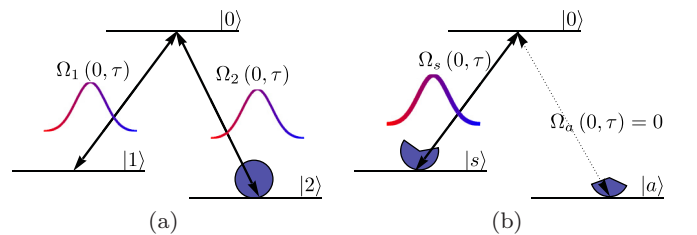


FIG. 2. (Color online) Boundary conditions given in (a) the original atomic basis and (b) the symmetric-antisymmetric basis. All of the atoms in the medium are initially prepared in the metastable state $|2\rangle$, which corresponds to a coherent superposition in the symmetric-antisymmetric basis given by the peak amplitudes ϑ_1 and ϑ_2 of the ingoing laser pulses.

where ϑ_1 and ϑ_2 are the peak amplitudes of the laser pulses at the entrance of the medium, and β is referred to as the speed of chirp. The parameters $\{\vartheta_1, \vartheta_2, \beta, \tau_\sigma\}$ in what follows are chosen in such a way that the conditions of adiabaticity [1] are fulfilled.

A. Symmetric-antisymmetric basis

For further investigation of the population dynamics in arbitrary segments of the medium, let us introduce a basis transformation on the atomic states and the electric-field modes adapted to the boundary conditions given in Eq. (9). This transformation leads us to the following symmetric-antisymmetric basis and effective Rabi frequencies:

$$|0\rangle, |s\rangle, |a\rangle = \left\{ |0\rangle, \frac{\vartheta_1|1\rangle + \vartheta_2|2\rangle}{\vartheta}, \frac{\vartheta_2|1\rangle - \vartheta_1|2\rangle}{\vartheta} \right\}, \quad (10a)$$

$$\begin{bmatrix} \Omega_s \\ \Omega_a \end{bmatrix} = \begin{bmatrix} (\vartheta_1\Omega_1 + \vartheta_2\Omega_2)/\vartheta \\ (\vartheta_2\Omega_1 - \vartheta_1\Omega_2)/\vartheta \end{bmatrix}, \quad (10b)$$

where $\vartheta = \sqrt{\vartheta_1^2 + \vartheta_2^2}$, and Ω_s and Ω_a give the couplings between the excited state $|0\rangle$ and the symmetric and anti-symmetric superpositional states $|s\rangle$ and $|a\rangle$, respectively. The Hamiltonian in this new basis becomes

$$\hat{H}_{sa}(\xi, \tau) = -\hbar \sum_{j \in \{s, a\}} [\Omega_j(\xi, \tau)|0\rangle\langle j| + \text{H.c.}] \quad (11)$$

The dynamics of the effective Rabi frequencies formally obeys the same differential equation as the original ones:

$$\partial_\xi \Omega_j = -i\alpha\rho_{j0}, \quad j \in \{s, a\}, \quad \rho_{j0} = \langle j|\hat{\rho}|0\rangle, \quad (12)$$

where $\vartheta_k \in \mathbb{R} \quad \forall k \in \{1, 2\}$ was utilized. Transforming the boundary conditions according to Eq. (10b) yields a set of boundary conditions which is more convenient for our purposes, as it only contains one ingoing laser mode [see Fig. 2(b)]:

$$\begin{bmatrix} \Omega_s(\xi = 0, \tau) \\ \Omega_a(\xi = 0, \tau) \end{bmatrix} = \begin{bmatrix} \vartheta \\ 0 \end{bmatrix} e^{-\tau^2(\frac{1}{2} + i\beta)}, \quad (13a)$$

$$\hat{\rho}(\xi, \tau \rightarrow -\infty) = \frac{1}{\vartheta^2} (\vartheta_2|s\rangle - \vartheta_1|a\rangle)(\vartheta_2\langle s| - \vartheta_1\langle a|). \quad (13b)$$

B. Rotating basis for adiabatic approximation

In the case of adiabatic evolution, the dynamics of the system can be well described by the analysis of the eigenstates of the interaction Hamiltonian. This is based on the fact that the evolution is slow (compared to the characteristic frequency defined by the inverse of the difference of the eigenenergies), thus the system follows the eigenstate in which it was initially prepared in [18,19]. We can only apply this approximation if the interaction Hamiltonian contains matrix elements that vary slowly in time (compared to the time scale of the interaction). For applying this approximation, it is important to use a basis in which the Hamiltonian of the system contains slowly varying matrix elements (in the scale of the interaction time).

We use an interaction picture for describing the atomic dynamics in each segment, applying the following rotating

basis vectors:

$$\{|0\rangle, |\tilde{s}\rangle, |\tilde{a}\rangle\} \equiv \{|0\rangle, |s\rangle e^{-i\phi_s(\xi, \tau)}, |a\rangle e^{-i\phi_a(\xi, \tau)}\}. \quad (14)$$

As a result, the time evolution is described in each segment by the following—slowly varying—Hamiltonian:

$$\begin{aligned} \hat{\mathcal{H}}_{sa}(\xi, \tau) = & -\hbar \sum_{j \in \{s, a\}} [\partial_\tau \phi_j(\xi, \tau) |\tilde{j}\rangle\langle \tilde{j}| \\ & + (|\Omega_j(\xi, \tau)\rangle\langle 0| + \text{H.c.})], \end{aligned} \quad (15)$$

where $\phi_j(\xi, \tau)$, $j \in \{s, a\}$, is the phase of the Rabi frequency $\Omega_j(\xi, \tau)$, $j \in \{s, a\}$ [cf. Eq. (3)]. Note that this transformation does not change the absolute values of the coefficients in the system's state vector.

III. PROPAGATION OF THE FC PULSE PAIR IN THE OPTICALLY THICK MEDIUM

In order to describe the collective behavior of the atom-laser system, we solve the system of differential equations (5) and (8) numerically. As already mentioned, the propagation equations for the Rabi frequencies are the same in both the original atomic and the transformed symmetric-antisymmetric basis except for the boundary conditions. Thus, it is easy to analyze the system in both coordinate systems. This is beneficial because the processes can be understood better in the transformed system, whereas it is important to have the results in the atomic basis where a possible measurement could be conducted.

The ingoing coupling fields that we consider are relatively strong, having a few 10π for pulse area of the Rabi frequencies Ω_1 and Ω_2 . The frequency modulation is chosen so that the pulses drive an adiabatic population transfer at the boundary of the medium, with a speed of chirp of $\beta = 7[1/\tau_\sigma^2]$. We would like to analyze a coherent population-transfer process in the medium, so the ingoing fields are considered to be short compared to the lifetime of the excited state $T_{|0\rangle} = 50\tau_\sigma$. For example, for a Rb^{87} atom having a lifetime of $\tau = 26.235$ ns, the pulse length should be approximately 2 ns, which means that a linear chirp speed of 28 GHz/ns and maximum Rabi frequencies in the order of 30 GHz would be needed.

A. Population dynamics induced by the FC pulse pair at the boundary of the medium ($\xi = 0$)

We first describe the interaction of the atoms with the Raman-resonant FC pulse pair at the boundary of the medium in the symmetric-antisymmetric basis. (The results are also valid approximately for an optically dilute medium.) It is easy to see from Eqs. (15) and (13) that the antisymmetric state $|\tilde{a}\rangle$ is an eigenstate of the Hamiltonian $\hat{\mathcal{H}}_{sa}(\xi = 0, \tau)$ since the coupling Ω_a is 0 for $\xi = 0$. The other metastable state $|\tilde{s}\rangle$ and the excited state $|0\rangle$ form a two-state atom coupled by a FC pulse which drives a rapid adiabatic passage from state $|\tilde{s}\rangle$ to the excited state $|0\rangle$, [2] (see Fig. 3). Since the antisymmetric state is decoupled from the excited state, it represents a dark state for the Raman-resonant FC pulses.

Similarly to the original case of constant-frequency matched pulses propagating in the medium of Λ atoms [36,40], the initial preparation of the atoms given in Eq. (13) does

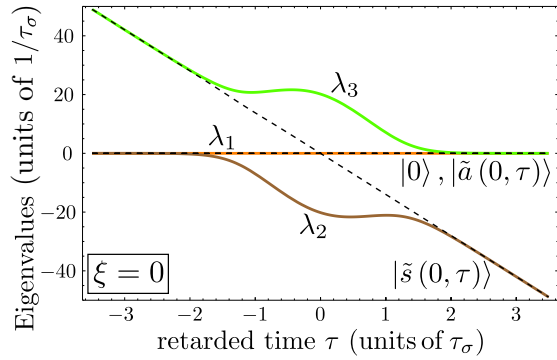


FIG. 3. (Color online) Eigenvalues of the Hamiltonian \hat{H}_{sa} [Eq. (15)], which describes the atom-laser system at the boundary of the medium ($\xi = 0$). The eigenvalues belonging to the diabatic states are plotted with dashed lines which correspond to states $|0\rangle$, $|\tilde{s}\rangle$, and $|\tilde{a}\rangle$, respectively. The eigenvalues of the adiabatic states are plotted with solid lines. The antisymmetric state $|\tilde{a}\rangle$ is an eigenstate of the Hamiltonian \hat{H}_{sa} with an eigenvalue of $\lambda_1 = 0$. The eigenstate belonging to λ_2 evolves from the excited state $|0\rangle$ to the symmetric state $|\tilde{s}\rangle$, while the other eigenstate belonging to λ_3 follows the inverse path ($|\tilde{s}\rangle \rightarrow |0\rangle$).

not coincide with the “dark” state. Based on the above considerations in the frame of the adiabatic approximation, the atoms at the boundary are expected to be transferred from a superposition of the metastable states $|\tilde{s}\rangle$ and $|\tilde{a}\rangle$ to a superposition of states $|\tilde{s}\rangle$ and the excited state $|0\rangle$. This result is in perfect agreement with the numerical solution of the master Eq. (5) at $\xi = 0$, which is depicted in Fig. 4.

In order to understand the laser propagation, it is important to analyze the time evolution of the coherences ρ_{0a} ($\xi = 0, \tau$) and ρ_{0s} ($\xi = 0, \tau$). We can easily understand the behavior of the absolute values of the coherences [see Fig. 5(a)] from the predictions of the adiabatic approximation. Since there is a complete population transfer between states $|s\rangle$ and $|0\rangle$, the absolute value of the coherence between them is 0 in the beginning and at the end of the interaction, and only differs from zero during the population transfer with a maximum

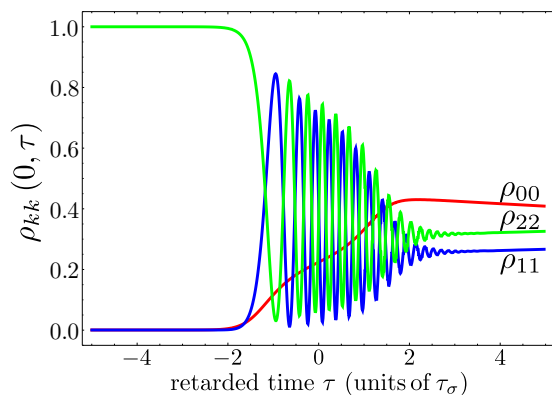


FIG. 4. (Color online) Dynamics of the atomic populations in the symmetric-antisymmetric basis at the boundary of the medium. The parameters used for the calculation are $\vartheta_1 = 15 [1/\tau_\sigma]$, $\vartheta_2 = 13.5 [1/\tau_\sigma]$, and $\beta = 7 [1/\tau_\sigma^2]$.

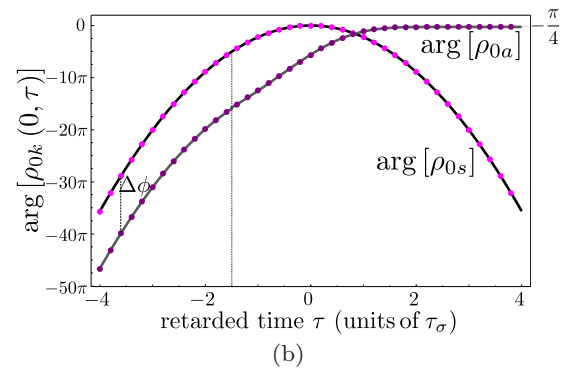
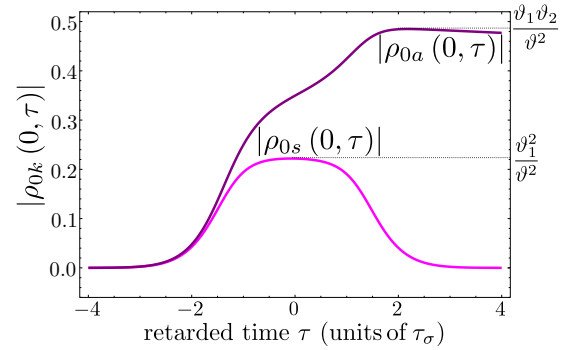


FIG. 5. (Color online) Time evolution of (a) the absolute value and (b) the phase of the atomic coherences at the boundary of the medium. For the absolute values of the coherences, the solid lines show the result of the numerical solution of the master equation for $\xi = 0$ using the same parameters that are given in Fig. 4. In the case of the phase of the coherences, the dots represent the result of the numerical solution, and the solid lines are the fitted functions: The function $\beta_0 + \beta_1 \tau^2$ is fitted on the values of $\rho_{0s}(\xi = 0, \tau)$ and on $\rho_{0a}(\xi = 0, \tau < -1.5\tau_\sigma)$ with the fitting parameters of $\{\beta_1^s = -6.99, \beta_0^s = 0.04\}$ and $\{\beta_1^a = -7.01, \beta_0^a = -34.35\}$, with $\beta_0^s - \beta_0^a = \Delta\phi = 10\pi + 0.95\pi$. A different function determines the time evolution of $\rho_{0a}(\xi = 0, \tau > -1.5\tau_\sigma)$: the function $\alpha_0 + \alpha_1 \exp(-\pi \exp[\alpha_2 \tau]/2)$ is fitted on the values, with the parameters $\{\alpha_0^{a0} = -0.78, \alpha_1^{a0} = -80.12, \alpha_2^{a0} = 0.76\}$.

value of $\vartheta_2^2/(2\vartheta^2)$. The time evolution of $|\rho_{0a}|$ is determined by the change of the population of the excited state $|0\rangle$ in time, since the population of state $|a\rangle$ does not change, as it is a dark eigenstate of the dressed atoms at the boundary of the medium. In parallel with the excitation of the atom, a coherence $\rho_{0a} = \vartheta_1 \vartheta_2 / \vartheta^2$ is established as a result of the interaction.

The time evolution of the phase of ρ_{0s} is determined by the phase of the coupling pulse Ω_s , which is set to be linearly chirped. It is clearly seen from Fig. 5(b) that the quadratic function $\beta_0 + \beta_1 \tau^2$ accurately fits the numerically calculated results of $\arg(\rho_{0s})$. The behavior of the phase of the coherence between the excited and the antisymmetric ground state ρ_{0a} is more complicated. Its time function starts as the same quadratic one as for ρ_{0s} , but the evolution changes approximately at $\tau = -1.5\tau_\sigma$, and it tends to a constant value as $\alpha_0 + \alpha_1 \exp(-\pi \exp[\alpha_2 \tau]/2)$.

B. Interaction of the propagating pulse pair and the atom inside the medium ($\xi > \xi_0$)

1. Laser field inside the medium

Let us now consider the time and space evolution of the effective Rabi frequencies Ω_s and Ω_a . In the symmetric-antisymmetric basis, only one, strong-coupling field (Ω_s) enters the medium of Λ atoms, which are prepared in a superposition of states $|a\rangle$ and $|s\rangle$ [cf. Eq. (13)]. In the course of the coherent transition process between the atomic states induced by Ω_s , a coherence is established between the antisymmetric and the excited state of the atoms close to the boundary, with a time function of its phase described in the previous section (cf. Fig. 5). This coherence generates the laser field Ω_a .

The time evolution of the absolute values and phases of the effective Rabi frequencies Ω_a and Ω_s at a given location inside the medium ($\xi = 40\xi_0$) is presented in Fig. 6. The coupling field Ω_s is only slightly modified during the propagation. The pulse envelope remains Gaussian with a good approximation after a propagation of multiple times of the absorption length ξ_0 . The change in the envelope of the effective Rabi frequency Ω_s is presented in the inset of Fig. 6(a). It can be observed that after $40\xi_0$ of propagation, the distortion from the boundary condition is less than 4% of the pulse area. The phase function with respect to time inside the medium also has the same character as at the boundary: the same quadratic function $\beta_0 + \beta_1 \tau^2$ fits the data in Fig. 6(a), so the frequency of this effective field changes linearly in time. Thus, the ingoing laser mode Ω_s preserves its initial properties during the propagation in the medium, with only a small loss in the pulse envelope.

However, the loss in the ingoing laser mode Ω_s allows for generating another mode Ω_a . The numerical calculations [see Fig. 6(b)] show that the character of the phase function of $\Omega_a(\xi, \tau)$ over time is at every location very similar to $\arg[\rho_{0a}(\xi = 0, \tau)]$, that is, the phase of the coherence between the symmetric and excited state over time. To be more specific, the same curve can be fit onto the numerical values of $\Omega_a(\xi, \tau) \forall \xi$ as in the case of the coherence ρ_{0a} at the boundary, with almost the same fitting parameters. The only differences are a shift of $-3\pi/2$ in the constant parameters α_0 and β_0 and a phase jump of π at every retarded-time point where $\Omega_a = 0$.

The behavior of the phase functions of Ω_s and Ω_a is understandable if we look at the coherences between the excited state and the antisymmetric and symmetric states— $\rho_{0a}(\xi, \tau)$ and $\rho_{0s}(\xi, \tau)$ —for the atoms at a typical inner location of the medium. It can be seen in Fig. 7 that although the absolute values of the coherences are smaller for atoms at $\xi \gg \xi_0$, the functions of their phases over time remain the same as they were at the boundary apart from phase jumps of π in the case of $\rho_{0a}(\xi, \tau)$. Since the macroscopic polarizations of the medium for the laser modes Ω_a and Ω_s are proportional to ρ_{0a} and ρ_{0s} , respectively, the result for the phases of the laser modes is plausible.

The phase jumps of π in the phase function of $\Omega_a(\xi \gg \xi_0)$ and also of $\rho_{0a}(\xi \gg \xi_0)$ occur when the quantities change their signs from positive to negative, or the other way around. This oscillatory behavior of the antisymmetric mode Ω_a and the coherence between the excited state and the antisymmetric state $|a\rangle$ can be understood as follows. The time evolution of

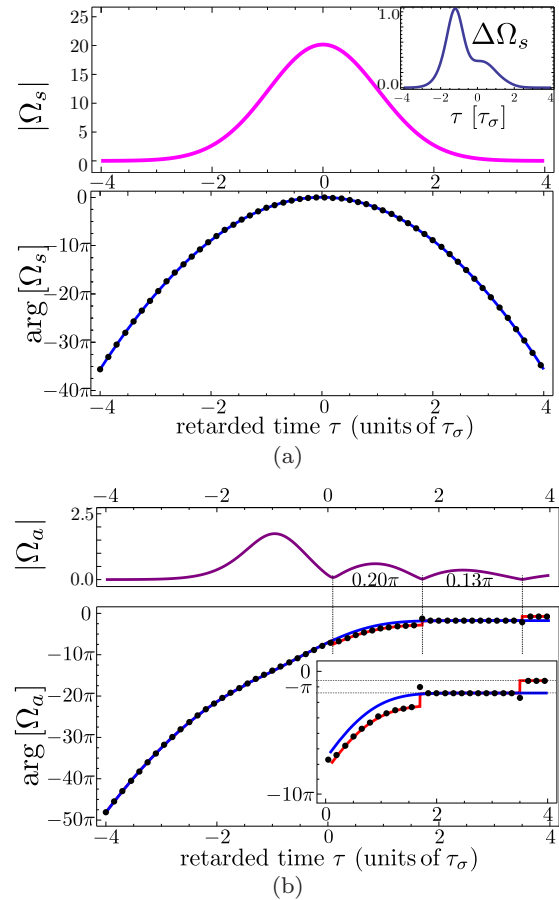


FIG. 6. (Color online) Absolute values and phases of the effective Rabi frequencies (a) Ω_s and (b) Ω_a as a function of the retarded time at a fixed space point inside the medium ($\xi = 40\xi_0$). Inset: Magnification of the plot showing the time evolution of the phases between $\tau = -1$ and $\tau = 4$. The parameters used for the calculation are the same as given in Fig. 4. The solid lines in the case of the absolute values and the dots in the case of the phases are the results of the numerical calculation. The same function—solid lines connecting the dots—fits on the calculations as the one that describes the phase of $\rho_{0a}(\xi = 0, \tau)$ (see Fig. 5), apart from “jumps” of $\pi/2$ which correspond to sign changes in the Rabi frequencies from positive to negative, or the other way around.

the phase of the antisymmetric mode is close to constant for approximately $\tau > 1.5\tau_\sigma$. This means that the excited and the antisymmetric ground states $|0\rangle$ and $|a\rangle$ are coupled by a train of small resonant pulses having nearly constant frequency, with a phase difference of π between the adjoining pulses. The pulse areas of these small pulses are much less than π , thus, as a result of the interaction with one pulse, a small part of a Rabi cycle proceeds between states $|0\rangle$ and $|a\rangle$. After this interaction, the process is reversed because of the next pulse, which has an opposite sign (π phase shift). Once this oscillation appears in the coherence ρ_{0a} , it affects the formation of the field Ω_a , and that is why the further this pulse propagates, the more small pulses appear (see Fig. 8).

To summarize, we found that—along with the almost-unchanged chirped Ω_s symmetric mode—an antisymmetric

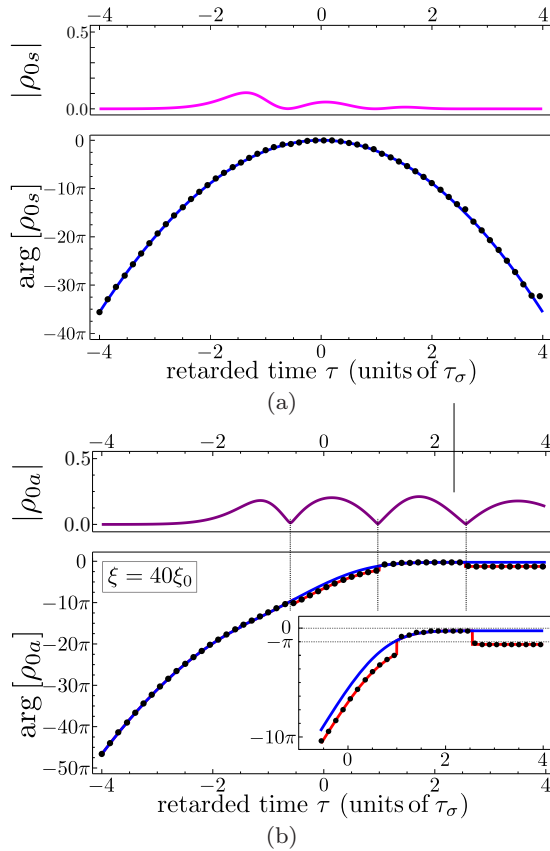


FIG. 7. (Color online) Time evolution of the absolute values and phases of the atomic coherences (a) ρ_{0s} and (b) ρ_{0a} inside the medium ($\xi = 40\xi_0$). Inset: Magnification of the plot showing the time evolution of the phases between $\tau = -1$ and $\tau = 4$. The solid lines in the case of the absolute values and the dots in the case of the phases are the results of the numerical calculation with the same parameters as in Fig. 4. The solid lines that connect the dots are functions fitted on the points. The same fitting functions were used as in the case of the coherences at the boundary (see Fig. 5) and the fitting parameters also proved to be the same. The only exception is β_0 , which needs to be shifted by π at the point where there is a jump in the data.

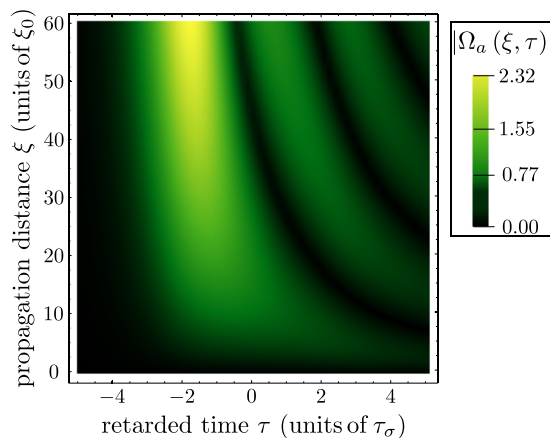


FIG. 8. (Color online) Absolute value of the effective Rabi frequency Ω_a as a function of the retarded-time coordinate and the propagation distance. The parameters used for the calculation are the same as in Fig. 4.

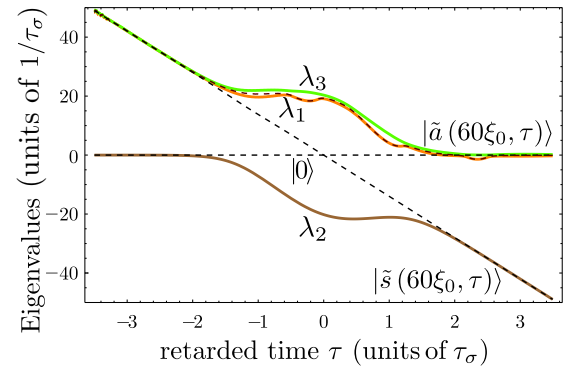


FIG. 9. (Color online) Eigenvalues of the Hamiltonian $\hat{\mathcal{H}}_{sa}$ [Eq. (15)], which describes the atom-laser system far from the boundary of the medium ($\xi = 40\xi_0$). The notations are the same as in Fig. 3.

mode Ω_a appears which is linearly chirped at the beginning and has a constant frequency at the end of the pulse.

2. The time evolution of the atoms' state inside the medium

Let us analyze the time evolution of the state of the atoms caused by the interaction with the above-described two modes Ω_s and Ω_a at a given location inside the medium. First we use the adiabatic approximation. The eigenvalues of the Hamiltonian $\mathcal{H}_{sa}(\xi, \tau)$ defined in Eq. (15) are presented in Fig. 9.

There is an obvious difference between this energy spectrum and the one of the interaction Hamiltonian characteristic to the atoms in the boundary (cf. Fig. 3). Namely, the eigenenergy of the diabatic state $|a\rangle$ has the constant value of zero and since $|a\rangle$ is completely uncoupled at the boundary, i.e., $\Omega_a(\xi = 0, \tau) = 0$, $|a\rangle$ is an adiabatic eigenstate as well, with a zero eigenvalue constant in time. In contrast, for atoms at inner locations $\xi \gg \xi_0$ of the medium, $\Omega_a(\xi \gg \xi_0, \tau)$ is, though small, nonzero and, as discussed in the previous section, has a nontrivial phase function over time. Since the time derivative of this phase is incorporated into the Hamiltonian $\hat{\mathcal{H}}_{sa}(\xi \gg \xi_0, \tau)$ in the interaction picture defined by the rotating basis (14), the diabatic state $|a\rangle$ here has a nontrivial time-dependent eigenvalue.

At the beginning of the interaction, the atoms are prepared in the superposition of the antisymmetric and symmetric diabatic states $|a\rangle$ and $|s\rangle$. As can be seen in Fig. 9, the eigenvalues of these adiabatic states correspond to the adiabatic eigenvalues λ_1 and λ_3 . Similar to the case at the boundary, the population, which was initially in state $|a\rangle$, remains there since λ_1 perfectly overlaps the diabatic energy of the antisymmetric state. On the other hand, the adiabatic eigenvalue λ_3 moves further from the diabatic energy of state $|s\rangle$ and remains close to the energy of $|a\rangle$. Based on the adiabatic theorem [18,19], we expect the population that was initially in the symmetric state $|s\rangle$ to be transferred into the antisymmetric state $|a\rangle$.

We also have to notice that these eigenstates— λ_1 and λ_3 —move close to the diabatic energy of the excited state $|0\rangle$ at the end of the interaction, for $\tau > 1.5\tau_\sigma$. We do not expect a large excitation of the atoms, however. Comparing Figs. 9 and 6(b), one realizes that the coupling Ω_a is very small for $\tau > 1.5\tau_\sigma$.

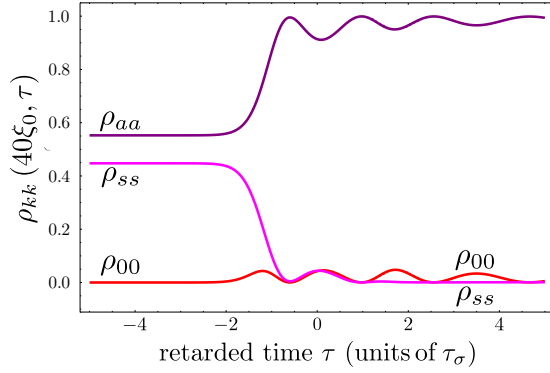


FIG. 10. (Color online) Dynamics of the populations of the atomic states inside the medium ($\xi = 40\xi_0$) in the symmetric-antisymmetric basis. The parameters used for the calculation are the same as given in Fig. 4.

The results of our numerical calculations—presented in Fig. 10—fit perfectly with the considerations in the adiabatic picture. That is, the majority of the population is transferred into the antisymmetric state $|a\rangle$ and the excitation of the atom is drastically reduced (it does not exceed 5% during the whole interaction). Thus, although complete population trapping is not established as in the case of the constant-frequency matched pulses [36], a quasidark state is created by the two modes Ω_s and Ω_a .

It is easy to see how the population-control process induced by the laser-pulse pair changes in the course of their propagation in the medium by looking at Fig. 11. This figure shows the populations of the states $|a\rangle$, $|s\rangle$ and $|a\rangle$ after the atoms' interaction with the laser pulses Ω_s and Ω_a . At the boundary and within one absorption length ξ_0 , a significant part of the population is transferred into the excited state. After a few absorption lengths, the excitation of the atom decreases, and although it shows an oscillatory behavior, it is always below 5% for atoms that are located at space positions $\xi > 6\xi_0$.

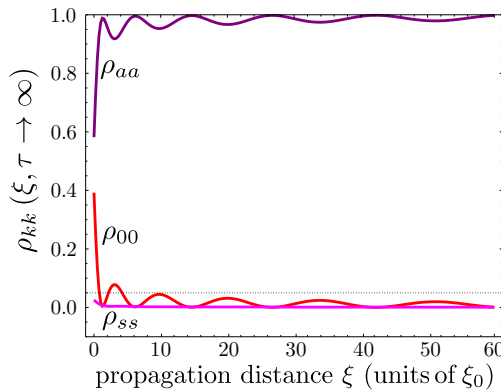


FIG. 11. (Color online) Final populations of the atoms at different space points ξ in the symmetric-antisymmetric basis. After a few absorption length ξ_0 of propagation, the pulse pair transfers the majority of the atomic population to the antisymmetric superposition of the ground states. The same parameters were used for the calculation as in Fig. 4.

We would like to point out here that the self-organization mechanism of the chirped-pulse pair is based on a population-transfer mechanism inside the medium that is substantially different from other cases found in the literature (see, e.g., [17,36] with references therein) dealing with propagation of constant-frequency pulses. Both of the latter are based on the fractional-STIRAP mechanism, where the final distribution of the population among the ground states is determined by the intensities of trailing edges of laser pulses [17]. In the case of the matched propagation of two constant-frequency pulses [36,40,41], the originally simultaneous laser pulses become shifted in time with respect to each other, allowing for a lossless propagation. Since oscillations can occur on the pulses' envelope, the final state can be significantly different for atoms at different locations. In [17], this problem is overcome by using adiabats as the boundary condition, but it has the disadvantage of the need for precise control of the ingoing pulse shape.

In our case, however, the adiabatic transfer occurs due to a different mechanism. This mechanism is based on the special time function of the antisymmetric mode Ω_a , which is generated by the medium. The adiabatic transfer results in the complete emptying of the symmetric state $|s\rangle$ and in the transfer of the majority of the population into the antisymmetric state $|a\rangle$.

C. Description of the system in the original basis

From the point of view of possible applications, it is important to “translate” our results in the symmetric-antisymmetric basis and with the effective couplings Ω_a and Ω_s into the original atomic basis. Figure 12 presents the population-transfer process induced by a pair of FC and constant-frequency pulses, respectively, in the original atomic basis at the boundary and at two given propagation lengths inside the medium ($\xi = 40\xi_0$ and $\xi = 60\xi_0$). The dynamics of the populations induced by the FC [Fig. 12(a)] and the constant-frequency pulse pair shows a conspicuous difference. This pronounced difference demonstrates well the different underlying physics, explained in detail in Sec. III B 2 by using the symmetric-antisymmetric basis.

On one hand, at the boundary, the Raman-resonant FC pulse pair induces a coherent population transfer, which distributes the population initially prepared in state $|2\rangle$ into a superposition of the three atomic states. The population of the excited state as a result of the interaction with the pulse pair is $\rho_{00} = \vartheta_2^2/\vartheta^2$, coinciding with the population of state $|s\rangle$ at the beginning of the interaction, while the population that remains in the ground states after the population transition process is $\rho_{11} = (\vartheta_1^2\vartheta_2^2)/\vartheta^2$ and $\rho_{22} = \vartheta_1^4/\vartheta^2$, respectively (which coincides with the initial population of the antisymmetric state $|a\rangle$).

Note that the requirement of the Raman resonance between the couplings plays an important role in the whole process under consideration. That is, a substantially different population evolution is induced by Raman-detuned couplings of the two allowed transitions [25], which leads to population transfer between the ground states, along with negligible excitation of the atom. This mechanism is rather similar for both a single

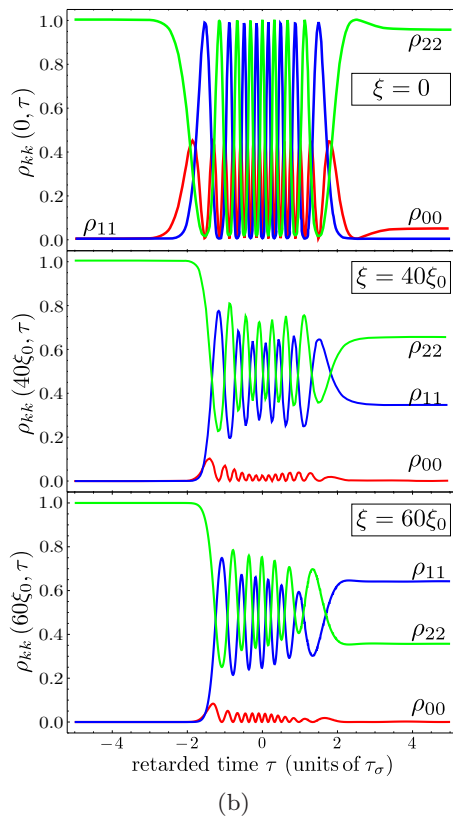
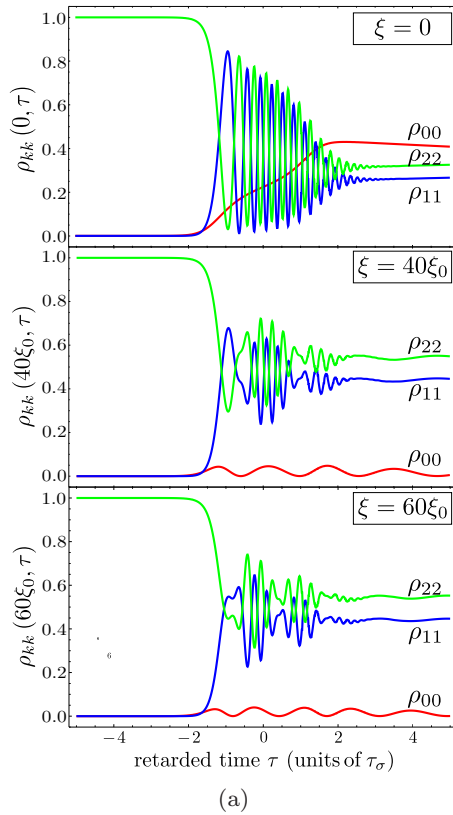


FIG. 12. (Color online) Evolution of the populations as a function of the retarded time τ induced by a pair of (a) chirped (FC) and (b) constant-frequency pulses at the boundary and at two typical propagation lengths inside the medium ($\xi = 40\xi_0$ and $\xi = 60\xi_0$). The parameters used for the numerical calculations are the same as in Fig. 4.

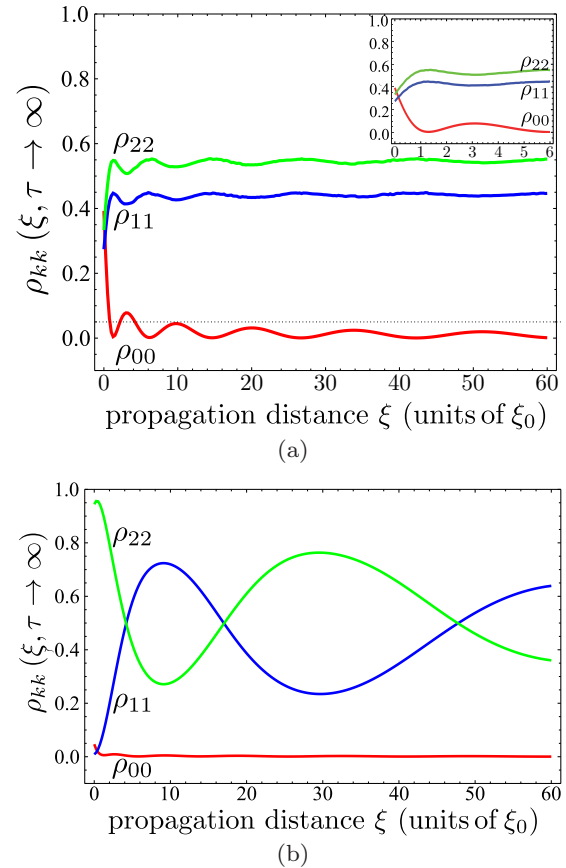


FIG. 13. (Color online) Final populations of the atoms at different space points ξ in the case of a (a) frequency chirped and (b) constant-frequency pulse pair. Inset: Final populations close to the boundary ($\xi \leq 6\xi_0$) for a FC pulse pair. After a few absorption length ξ_0 of propagation, the FC pulse pair transfers the majority of the atomic population to the antisymmetric superposition of the ground states, while in the case of the matched pulses having constant frequency, the final state strongly varies with ξ . The parameters used for the calculations are $\vartheta_1 = 15 [1/\tau_\sigma]$, $\vartheta_2 = 13.5 [1/\tau_\sigma]$, $\beta = 7 [1/\tau_\sigma^2]$, and $\beta = 0$, respectively.

atom and the atoms in an optically thick medium, taking into account propagation of the interacting laser pulses.

In contrast, in the present case of Raman-resonant coupling, both the pulse envelopes and the time function of the phases of the pulses are modified by the interaction with the medium after a short propagation length. The modification takes place in such a way that instead of exciting the atom, the pulses drive the main part of the population into the $(\vartheta_2|1\rangle - \vartheta_1|2\rangle)/\vartheta$ superposition of the ground states (see Fig. 13).

On the other hand, the constant-frequency pulses induce a Rabi oscillation between the excited state and the superposition of states $|1\rangle$ and $|2\rangle$, which corresponds to the antisymmetric state $|a\rangle$. Similarly to the FC case, the constant-frequency pulses become “matched” [36] (cf. Sec. III B 2), that is, the excitation of the atoms is drastically reduced inside the medium.

Note that neither in the FC nor in the constant-frequency case is all the population transferred to the antisymmetric superposition. In the case of the FC pulse pair, it is the excited state which is slightly populated, but in the weakly decaying regime under consideration, this does not significantly

disturb the preparation of the medium into a well-defined superposition state controlled by the peak Rabi frequencies of the ingoing pulses, as shown in Fig. 13(a). Figure 13(b) demonstrates the advantage of using FC pulses. Since the matched pulses having constant frequencies transfer different (though small) amounts of population into the symmetric superposition $|s\rangle$ in atoms at different locations ξ , the induced population distribution among the atomic states changes significantly as a function of ξ [see Figs. 12(b) and 13(b)]. We would like to emphasize that the difference in the state of the medium created by the chirped and the constant-frequency pulse pair is due to the different underlying physics, explained in detail in Sec. III B 2.

The Rabi frequencies can be expressed by the symmetric and antisymmetric Rabi frequencies as

$$\Omega_1 = \frac{\vartheta_1}{\vartheta} \Omega_s + \frac{\vartheta_2}{\vartheta} \Omega_a, \quad (16a)$$

$$\Omega_2 = \frac{\vartheta_2}{\vartheta} \Omega_s - \frac{\vartheta_1}{\vartheta} \Omega_a. \quad (16b)$$

As the pulses propagate in the medium, energy is transferred from Ω_2 (which couples the transition where the atoms are prepared) to Ω_1 . Since Ω_a is one order of magnitude weaker than Ω_s , even after propagation length of many times ξ_0 (cf. Fig. 6), the distortion is small. In this sense, it can be stated that the FC pulse pair propagates quasitransparently and that it can prepare a well-defined coherent superposition of the ground states in an extended medium of relatively large optical depth (see Fig. 14).

IV. SUMMARY

We have analyzed the propagation of a pair of Raman-resonant, linearly frequency-modulated strong laser pulses in an optically thick medium, which is modeled as a motionless and noninteracting ensemble of Λ atoms. We have demonstrated that quasiloessless propagation of FC pulses is possible not only when the medium is initially prepared in a quasidark state [29], but through a *matching* effect between the two pulses. Namely, although the Raman-resonant pulse pair causes a significant excitation in the atoms close to the boundary of the medium, the excitation of the atoms becomes negligible in the medium at larger propagation length. Excitation of the atoms near the boundary of the medium, however, plays an important role in the generation of a macroscopic polarization, which interaction with the FC pulses results in the matched quasiloessless propagation of the pulses in the optically thick medium.

By analyzing the dressed states of the atoms, we have demonstrated that the FC pulse pair induces a population-transfer mechanism substantially different from the transfer process typical for the matched pulses having constant carrier frequency. The FC pulse pair, in the course of its propagation, transfers the majority of the atoms of the medium into approximately the same coherent superposition of their ground states. In contrast, the population distribution among the ground states induced by the constant-frequency pulse pair may change significantly at different locations in the medium.

We have shown that the composition of the coherent superposition, established by the propagating FC pulse pair,

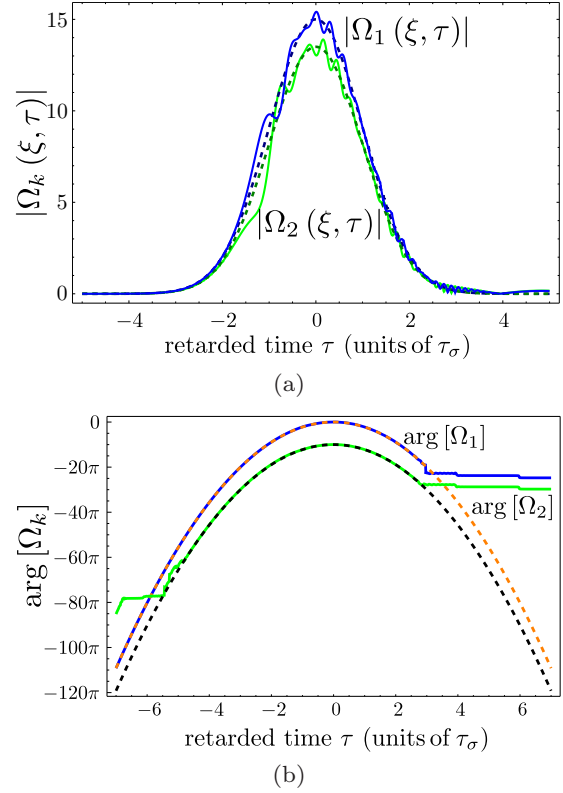


FIG. 14. (Color online) (a) Envelope functions of the pulses at the boundary (dashed lines) and at $\xi = 40\xi_0$ (solid lines). (b) The phases of the Rabi frequencies as a function of the retarded time τ at the boundary (dashed lines) and inside the medium (solid lines). The same parameters were used for the numerical calculation as given in the caption of Fig. 4.

depends on the peak amplitudes of these laser pulses at the boundary of the medium. Therefore, the magnitude of the coherence created by the interaction may be tuned by parameters which are easily controllable experimentally.

The obtained results, especially those concerning the robust creation of coherence between atomic metastable (ground) states in a spatially extended, optically thick medium, may find important applications in schemes of frequency conversion through nonlinear optical mixing processes, as well as in other nonlinear processes where the initial preparation of an extended medium in a coherent superposition state is needed [9–16].

Another possible application of the process may be in the realm of quantum communication, where chirped pulses have been proven useful in photon-echo-based quantum memories [42]. For this direction of usage, the analysis of the propagation mechanism in the presence of inhomogeneous broadening is needed, which will be the subject of our next paper.

ACKNOWLEDGMENTS

This work was funded by the Research Fund of the Hungarian Academy of Sciences (OTKA) under Contract No. NN 78112; by Grant No. ELI- 09-1-2010-0010; and by the TÁMOP 4.2.4.A/2-11-1-2012-0001 “National Excellence Program.”

- [1] K. Bergmann, H. Theuer, and B. W. Shore, *Rev. Mod. Phys.* **70**, 1003 (1998).
- [2] Nikolay V. Vitanov, Thomas Halfmann, Bruce W. Shore, and Klaas Bergmann, *Annu. Rev. Phys. Chem.* **52**, 763 (2001).
- [3] Petr Král, Ioannis Thanopoulos, and Moshe Shapiro, *Rev. Mod. Phys.* **79**, 53 (2007).
- [4] J. B. Watson, A. Sanpera, X. Chen, and K. Burnett, *Phys. Rev. A* **53**, R1962 (1996).
- [5] R. R. Jones, *Phys. Rev. Lett.* **75**, 1491 (1995).
- [6] Z. Kis and E. Paspalakis, *Phys. Rev. A* **68**, 043817 (2003).
- [7] A. Eilam, A. D. Wilson-Gordon, and H. Friedmann, *Phys. Rev. A* **73**, 053805 (2006).
- [8] L. J. Wang, A. Kuzmich, and A. Dogariu, *Nature (London)* **406**, 277 (2000).
- [9] M.O. Scully, *Phys. Rep.* **219**, 191 (1992).
- [10] M. O. Scully, S. Y. Zhu, and H. Fearn, *Z. Phys. D* **22**, 471 (1992).
- [11] J. Mompert and R. Corbali, *J. Opt. B* **2**, R7 (2000).
- [12] A. S. Zibrov, M. D. Lukin, L. Hollberg, D. E. Nikonov, M. O. Scully, H. G. Robinson, and V. L. Velichansky, *Phys. Rev. Lett.* **76**, 3935 (1996).
- [13] M. D. Lukin, S. F. Yelin, A. S. Zibrov, and M. O. Scully, *Laser Phys.* **9**, 759 (1999).
- [14] R. Kolesov, M. O. Scully, and O. Kocharovskaya, *Phys. Rev. A* **74**, 053820 (2006).
- [15] V. A. Sautenkov, M. D. Lukin, C. J. Bednar, I. Novikova, E. Mikhailov, M. Fleischhauer, V. L. Velichansky, G. R. Welch, and M. O. Scully, *Phys. Rev. A* **62**, 023810 (2000).
- [16] A. Wojciechowski, E. Corsini, J. Zachorowski, and W. Gawlik, *Phys. Rev. A* **81**, 053420 (2010).
- [17] Victor V. Kozlov and Ekaterina B. Kozlova, *Opt. Commun.* **282**, 892 (2009).
- [18] J. Oreg, F. T. Hioe, and J. H. Eberly, *Phys. Rev. A* **29**, 690 (1984).
- [19] D. Grischkowsky, *Phys. Rev. A* **14**, 802 (1976).
- [20] U. Gaubatz, P. Rudecki, S. Schiemann, and K. Bergmann, *J. Chem. Phys.* **92**, 5363 (1990).
- [21] R. G. Unanyan, B. W. Shore, and K. Bergmann, *Phys. Rev. A* **63**, 043401 (2001).
- [22] Thorsten Peters, Leonid P. Yatsenko, and Thomas Halfmann, *Phys. Rev. Lett.* **95**, 103601 (2005).
- [23] N. V. Vitanov, K.-A. Suominen, and B. W. Shore, *J. Phys. B* **32**, 4535 (1999).
- [24] Ignacio R. Solá, Vladimir S. Malinovsky, Bo Y. Chang, Jesus Santamaria, and Klaas Bergmann, *Phys. Rev. A* **59**, 4494 (1999).
- [25] G. P. Djotyan, J. S. Bakos, Zs. Sörlei, and J. Szigeti, *Phys. Rev. A* **70**, 063406 (2004).
- [26] G. P. Djotyan, J. S. Bakos, G. Demeter, Zs. Sörlei, J. Szigeti, and D. Dzsotjan, *J. Opt. Soc. Am. B* **25**, 166 (2008).
- [27] Nora Sandor, Joseph S. Bakos, Zsuzsa Sörlei, and Gagik P. Djotyan, *J. Opt. Soc. Am. B* **28**, 2785 (2011).
- [28] M. Fleischhauer, *Opt. Express* **4**, 107 (1999).
- [29] G. Demeter, D. Dzsotjan, and G. P. Djotyan, *Phys. Rev. A* **76**, 023827 (2007).
- [30] Paul Siddons, Charles S. Adams, and Ifan G. Hughes, *J. Phys. B* **45**, 124009 (2012).
- [31] J. P. Marangos, *J. Mod. Opt.* **45**, 471 (1998).
- [32] M. Fleischhauer and M. D. Lukin, *Phys. Rev. Lett.* **84**, 5094 (2000).
- [33] J. Wang, L. B. Kong, X. H. Tu, K. J. Jiang, K. Li, H. W. Xiong, Yifu Zhu, and M. S. Zhan, *Phys. Lett. A* **328**, 437 (2004).
- [34] S. E. Harris, *Phys. Rev. Lett.* **70**, 552 (1993).
- [35] R. Grobe, F. T. Hioe, and J. H. Eberly, *Phys. Rev. Lett.* **73**, 3183 (1994).
- [36] S. E. Harris and Zhen-Fei Luo, *Phys. Rev. A* **52**, R928 (1995).
- [37] G. P. Djotyan, J. S. Bakos, and Zs. Sörlei, *Phys. Rev. A* **64**, 013408 (2001).
- [38] L. C. Allen and J. H. Eberly, *Optical Resonance and Two-Level Atoms*, Dover Books on Physics Series (Dover, New York, 1975).
- [39] Alejandro A. Duarte and Hernán G. Solari, *Opt. Commun.* **144**, 99 (1997).
- [40] S. E. Harris, *Phys. Rev. Lett.* **72**, 52 (1994).
- [41] Stephen E. Harris, *Phys. Today* **50**, 36 (1997).
- [42] V. Damon, M. Bonarota, A. Louchet-Chauvet, T. Chaneliere, and J.-L. Le Gouet, *New J. Phys.* **13**, 093031 (2011).